



Textural and chemical evolution of a fractionated granitic system: the Podlesí stock, Czech Republic

Karel Breiter^{a,*}, Axel Müller^b, Jaromír Leichmann^c, Ananda Gabašová^a

^a*Czech Geological Survey, Geologická 6, CZ-15200 Praha 5, Czech Republic*

^b*Natural History Museum, Dept. Mineralogy, Cromwell Road, London SW75BD, United Kingdom*

^c*Department of Geology and Paleontology, Masaryk University, Kotlářská 2, CZ-61137 Brno, Czech Republic*

Received 17 March 2003; accepted 9 September 2004

Available online 18 November 2004

Abstract

The Podlesí granite stock (Czech Republic) is a fractionated, peraluminous, F-, Li- and P-rich, and Sn, W, Nb, Ta-bearing rare-metal granite system. Its magmatic evolution involved processes typical of intrusions related to porphyry type deposits (explosive breccia, comb layers), rare-metal granites (stockscheider), and rare metal pegmatites (extreme F–P–Li enrichment, Nb–Ta–Sn minerals, layering). Geological, textural and mineralogical data suggest that the Podlesí granites evolved from fractionated granitic melt progressively enriched in H₂O, F, P, Li, etc. Quartz, K-feldspar, Fe–Li mica and topaz bear evidence of multistage crystallization that alternated with episodes of resorption. Changes in chemical composition between individual crystal zones and/or populations provide evidence of chemical evolution of the melt. Variations in rock textures mirror changes in the pressure and temperature conditions of crystallization. Equilibrium crystallization was interrupted several times by opening of the system and the consequent adiabatic decrease of pressure and temperature resulted in episodes of nonequilibrium crystallization. The Podlesí granites demonstrate that adiabatic fluctuation of pressure (“swinging eutectic”) and boundary-layer crystallization of undercooled melt can explain magmatic layering and unidirectional solidification textures (USTs) in highly fractionated granites.

© 2004 Elsevier B.V. All rights reserved.

Keywords: Granite; Breccia; UST; Magmatic layering; Feldspars; Quartz

1. Introduction

Granitic pegmatites, tin granites and subvolcanic porphyry deposit-related intrusions represent three

different results of fractionation of silicic magmas. For porphyry-related intrusions, evolution in an open system was established a long time ago, but granites and pegmatites were, until the 1980s, considered to be products of slow closed-system crystallization. However, many structural as well as compositional links among these systems have been found recently. Explosive brecciation in a subvolcanic tin–granite

* Corresponding author. Tel.: +420 251085508; fax: +420 251818748.

E-mail address: breiter@cgu.cz (K. Breiter).

was recognised in Krušné Hory/Erzgebirge and Cornwall (Schust and Wasternack, 1972; Allman-Ward et al., 1982). Magmatic layering with crystals oriented perpendicular to the individual layers (unidirectional solidification texture, UST¹; Shannon et al., 1982) was found to be typical of subvolcanic granitic stocks with associated Sn, W and Mo mineralisation. Such layering is typically parallel to the contact of the intrusions and is composed of layers of euhedral quartz crystals alternating with layers of fine-grained aplite. A special type of UST are comb quartz layers (Kirkham and Sinclair, 1988). Simple magmatic layering with orientation of minerals parallel to the layers is common in aplite–pegmatite bodies (e.g., Duke et al., 1992; Breaks and Moore, 1992; Morgan and London, 1999), but in true granites it is much less abundant (Zaraisky et al., 1997). Calculations based on conductive cooling of some flat aplite–pegmatite dykes intruded into relatively cool country rocks suggest a rapid rate of crystallization (5 to 340 days for 1- to 8-m-thick dykes; Webber et al., 1999).

All these phenomena suggest crystallization of granitic magma in an open system involving rapid changes in p – T – X conditions. Fractionated granitic and pegmatitic systems have been intensively studied during the last two decades and a considerable amount of new natural and experimental data are now available (cf. London, 1990, 1992, 1995, 1996). Magmatic layering has been explained by several models (Brigham, 1983; London, 1992, 1999; Balashov et al., 2000; Fedkin et al., 2002) with strong undercooling and/or a sudden decrease of pressure having a crucial role. Nevertheless, there are few well-exposed natural examples that verify these experimental predictions.

¹ In this paper, we use the term “layering” or “layered rock” for rocks with layers differing in grain size and/or mineral composition regardless of the orientation of individual crystals. The term “UST” (unidirectional solidification texture) refers to a layer composed of crystals oriented perpendicularly to the plain of layering and the term “comb mineral” is an oriented crystal within a UST layer. “Snow-ball quartz” (late quartz phenocryst with abundant albite laths arranged concentrically along its growth planes) is considered to be an igneous texture. “Snow-ball fabric” applies here also to comb orthoclase. “Stockscheider” is an old German mining term for K-feldspar-dominated pegmatite at the upper contact of some tin-bearing granites (in the geological literature since 1865; Jarchovský, 1962, and references therein).

One of these is the Podlesí granite stock (Czech Republic)—an extremely fractionated, peraluminous, F-, Li- and P-rich, and Sn, W, Nb, Ta-bearing rare-metal granite with an early intrusive/explosive breccia, marginal pegmatite, feldspar- and zinnwaldite-dominated USTs, and late intra-dyke brecciation. Major minerals bear evidence for multistage crystallization that alternated with episodes of resorption. Changes in chemical composition between individual crystal zones and/or populations provide evidence for the chemical evolution of the melt, while variation in rock textures mirrors changes in the pressure and temperature conditions of crystallization.

2. Geologic setting and shape of the intrusion

The Podlesí granite stock (0.1 km²) is situated in the western part of the Krušné Hory Mts., Czech Republic. It is the youngest intrusion (313 to 310 Ma) of the multistage late-Variscan tin-specialised Eibenstock-Nejdek pluton that intruded Ordovician phyllites and a Variscan biotite granite. Several boreholes drilled by the Czech Geological Survey penetrate the intrusion in a >400-m-long vertical section (Breiter, 2002).

The overall shape of the intrusion is tongue-like (Fig. 1). The stock consists primarily of an albite–protolithionite–topaz granite (stock granite), which can be divided into two subfacies. The “upper facies” forms the uppermost 30- to 40-m-thick carapace of the stock and is fine-grained and porphyritic. The “lower facies” comprising the main part of the stock is medium-grained and equigranular. The uppermost part of the cupola is bordered by a 50-cm-thick marginal pegmatite (stockscheider).

In the uppermost 100 m, the stock granite has been intruded by several subhorizontal dykes of albite–zinnwaldite–topaz granite (dyke granite). Upper and lower contacts of the dykes are sharp and slightly uneven. Thin (mm- to cm-scale) steeply dipping apophyses are found around the larger dykes. The biggest dyke (hereafter referred to as “major dyke”) is 7 m thick. Its western part is well exposed and shows prominent magmatic layering with USTs. In the eastern part, a late-magmatic intra-dyke breccia is also found. The dyke generally dips 5° to 10° to the southwest, with the eastern part of the dyke representing the uppermost apical part. The western and eastern

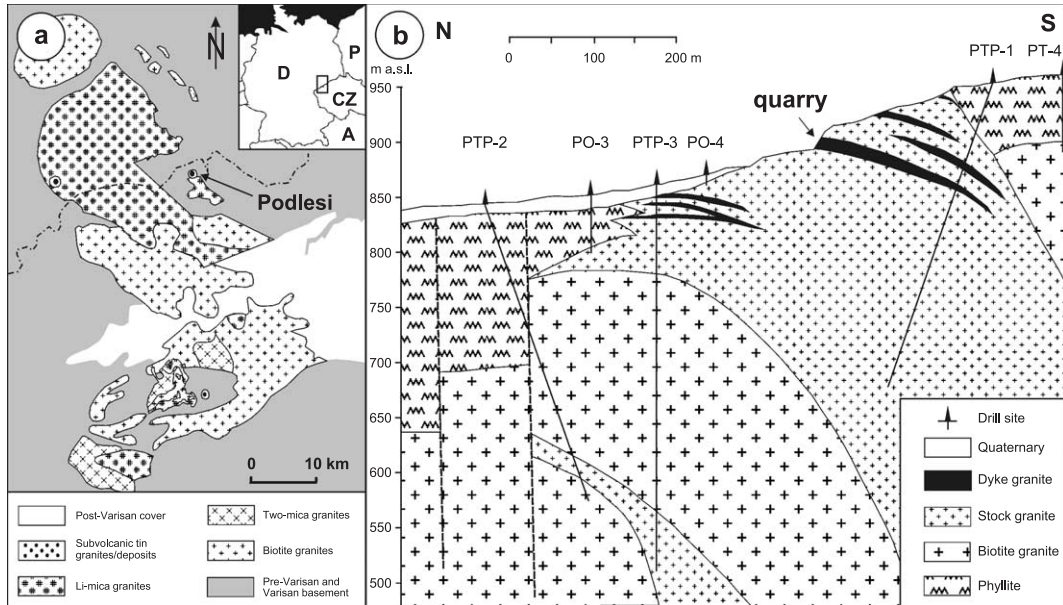


Fig. 1. (a) Simplified geological map of the Western Krušné Hory/Erzgebirge Mountains and location of the Podlesí granite system. Inset shows area relative to eastern Europe; A—Austria, CZ—Czech Republic, D—Germany, P—Poland. (b) Geological cross section through the Podlesí granite stock. The “major dyke” crops out in the quarry.

parts of the dyke are here termed the proximal and distal portions of the dyke, respectively.

3. Data

We present scanning electron microscope and optical cathodoluminescence as well as mineral chemical and whole-rock geochemical data on the various rock types and mineral assemblages of the Podlesí stock. The pertinent analytical methods are described in Appendix A.

3.1. Whole-rock chemistry

Both facies of the stock granite are strongly peraluminous (A/CNK 1.15–1.25; including Li, Rb and Cs as charge balancing cations in the denominator, the peraluminosity index will decrease to 1.1–1.2) and, in comparison with common Ca-poor granites, enriched in incompatible elements such as Li, Rb, Cs, Sn, Nb, U, W, and poor in Mg, Ca, Sr, Ba, Fe, Sc, Zr, Pb, and V (Breiter, 2002). They are also rich in P (0.4–0.8 wt.% P_2O_5) and F (0.6–1.8 wt.%). A high degree of magmatic fractionation is demonstrated by

low K/Rb (22–35) and Zr/Hf (12–20) and high U/Th (4–7). The dyke granite is even more enriched in Al (A/CNK 1.2–1.4; 1.1–1.3 taking Li, Rb and Cs into account), P (0.6–1.5 wt.% P_2O_5), F (1.4–2.4 wt.%), Na, Rb, Li, Nb, Ta, and depleted in Si, Zr, Sn, W and REE. The K/Rb (14–20) and Zr/Hf (9–13) ratios are lower than in the stock granite (Table 1).

All the Podlesí granite types are rich in P, which shows a positive correlation with F, Al, Li, Rb, Nb, Ta and peraluminosity, and a negative correlation with Si, Zr and Sn. They are also relatively B-poor (20–60 ppm). However, tourmalinisation evolved in phyllite in a broader contact aureole of the granite stock suggests that B content in the melt may have been substantially higher.

A high degree of fractionation is documented also by high concentrations of rare metals. Nb and Ta are more abundant in the dyke granite (50–95 ppm Nb and 30–55 ppm Ta) than in the stock granite (25–50 and 10–25 ppm, respectively). On the other hand, contents of Sn and W are distinctly higher in the stock granite (10–50 ppm Sn, 20–80 ppm W) than in the dyke granite (5–20 and 35–60 ppm, respectively). The REE contents of the stock granite are low and chondrite-normalised patterns relatively flat [(Ce/

Table 1
Chemical composition of the granites of the Podlesí system

No.	3361	3436	3416	3417	3415	3414	3413	3739	3742	3741
Locality	SW contact of the body	Borehole PTP1 depth 200 m	Old quarry, proximal dyke				Outcrop, distal dyke			
Rock	Stockscheider	Stock granite	Top of the dyke	Kfs-rich UST	Lamin. dyke	Lamin. dyke	Base of the dyke	Homogen. dyke	Breccia fragm.	Breccia matrix
SiO ₂	74.78	72.52	70.10	66.54	70.72	70.66	72.52	72.10	62.53	67.90
TiO ₂	0.05	0.02	0.02	0.02	0.02	0.02	0.01	0.01	0.04	0.03
Al ₂ O ₃	13.80	15.13	15.77	17.79	16.03	15.89	15.98	15.42	18.65	17.31
Fe ₂ O ₃	0.414	0.345	0.111	0.15	0.118	0.166	<0.01	0.23	0.37	0.22
FeO	0.464	0.58	0.674	0.945	0.551	0.822	0.55	0.42	1.84	0.74
MnO	0.026	0.023	0.036	0.046	0.037	0.08	0.041	0.054	0.122	0.053
MgO	0.05	0.05	0.02	0.02	0.01	0.03	0.04	0.02	0.01	0.02
CaO	0.43	0.44	0.43	0.39	0.27	0.28	0.17	0.18	0.1	0.06
Li ₂ O	0.033	0.181	0.332	0.442	0.293	0.432	0.29	0.348	1.502	0.608
Na ₂ O	3.60	3.77	4.10	2.90	4.34	4.10	4.89	4.92	3.84	5.46
K ₂ O	4.23	4.32	4.25	6.42	4.22	3.80	3.51	3.61	4.31	3.90
P ₂ O ₅	0.397	0.46	1.03	0.80	0.79	0.859	0.524	0.549	1.272	0.996
F	0.505	1.25	1.31	1.72	1.38	1.82	1.33	1.233	3.822	1.529
H ₂ O+	0.884	0.966	1.34	1.55	0.882	1.06	0.90	0.80	1.34	1.15
H ₂ O–	0.23	0.10	0.21	0.12	0.08	0.10	0.14	0.07	0.11	0.05
Total	99.72	99.63	99.22	99.16	99.18	99.38	100.36	99.96	99.85	100.03
Ba	23	4	13	12	5	24	9	1	1	5
Bi	3	3	8	49	57	24	8	9	22	20
Cs	56	82	143	198	128	170	159	150	343	172
Ga	31	39	60	56	50	51	52	59	69	74
Hf	2.0	1.9	4.6	2.2	3.5	3.1	1.8	2.1	4.2	3.5
Nb	56	35	99	89	90	83	55	59	153	104
Pb	10	4	<2	8	<2	2	<2	<2	3	<2
Rb	551	1260	2162	3025	2084	2175	1970	2370	4380	2870
Sn	18	69	29	31	41	27	34	24	78	27
Sr	16	27	182	99	86	102	60	11	15	14
Ta	19	15	68	54	53	54	20	20	65	42
Th	7.5	5.3	5.4	12.1	6	5.8	6.3	7.3	11.4	6.9
Tl	2.5	2.9	4.3	6.2	4.3	4	3.5	1.7	6.3	3.4
U	43	35	47	44	37	35	20	20	47	32
W	24	38	49	55	49	63	23	30	93	48
Zn	47	43	79	97	60	69	73	69	224	100
Zr	22	25	34	13	29	24	18	14	37	34

Major elements (in wt.%) determined at the Czech Geological Survey by wet chemistry. Nb, Pb, Rb, Sn, Sr, Zn and Zr (in ppm) by XRF at the Czech Geological Survey, the other trace elements (in ppm) by ICP-MS in ACMElab in Vancouver, Canada.

Yb)_N=4–5] with distinct negative Eu anomalies. The dyke granite is even more depleted in REE and shows the lanthanide tetrad effect (Breiter et al., 1997).

3.2. Textural evidence of crystallization conditions

3.2.1. Stockscheider

At Podlesí, a 30- to 50-cm-thick stockscheider is found along the southern and southwestern margin of the body. It is composed of large prismatic microcline

crystals oriented perpendicular to the contact plane of the granite with phyllite. The space between individual microcline crystals is filled with albite-rich fine-grained matrix and, in places, with large grains of milky quartz. The stockscheider changes downwards into fine-grained stock granite. In a transition zone several metres thick, the granite contains K-feldspar crystals about 5 cm long and 1 to 2 cm thick and local layers with comb quartz. Phenocrysts of quartz and microcline within the stockscheider are markedly

altered. In one sample, fragments of large microcline crystals are cemented by fine-grained granitic matrix containing fragmented topaz crystals (Fig. 2A). This

suggests that crystallization of at least some parts of the stockscheider predated the first episode of brecciation (see below).

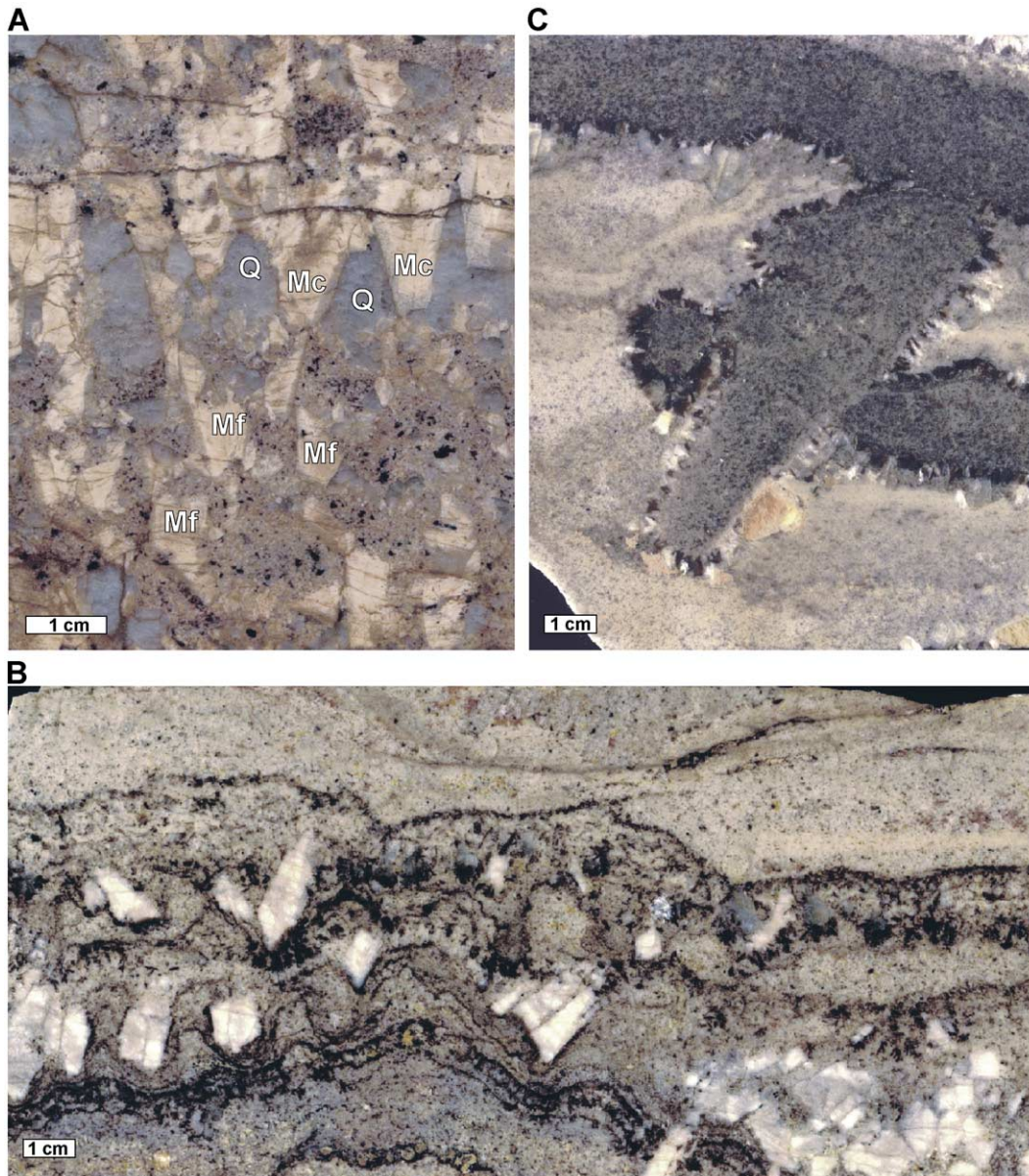


Fig. 2. Macrotextures in the Podlesí stock. (A) Stockscheider, individual crystals of microcline (Mc) in the upper part of the sample have grown downwards, space between the crystals is filled by milky quartz (Q). In the lower part, fragments of microcline crystals (Mf) have been cemented with fine-grained granitic matrix. (B) K-feldspar (orthoclase) dominated UST layer near the upper contact of the major dyke. Light laminae are composed of quartz, albite, K-feldspar and topaz, dark laminae are pure zinnwaldite. (C) Intra-dyke breccia: horizontal mica-rich facies in the upper part of the sample is rimmed with quartz-zinnwaldite UST at its lower margin. Fragments of the mica-rich facies in the central part of the sample are rimmed by zinnwaldite-orthoclase UST. Space between the fragments is filled with albite-quartz-topaz matrix. In all these cases, direction of crystallization is downwards.

Table 2
Petrography of the major dyke in Podlesí (cf. Fig. 3)

No. of layers	Thickness (cm)	Description
1	1	Very fine-grained granite with sharp hanging wall contact.
2	2–3	K-feldspar-dominated UST layer, columnar orthoclase crystals overgrown by fine-grained granitic matrix.
3	30	Thin laminae consisting of quartz, albite and P-rich K-feldspar in different proportions. Zinnwaldite is partly disseminated, partly concentrated in thin nearly monomineralic laminae. Contacts of the laminae are generally irregular and/or folded. Small-scale protrusions of not fully crystallized material in the hanging wall of some laminae are present.
4	10	Pegmatite-like UST layer consisting of large (up to 7×1 cm) oriented subhedral columns of twinned K-feldspar crystals rimmed by fan-like aggregates of zinnwaldite (Fig. 2B). The fine-grained granitic matrix is composed of anhedral quartz, K-feldspar, albite and zinnwaldite. Topaz is common. This layer is the most enriched in Nb–Ta minerals.
5	15	Laminated fine-grained layer with scarce individual oriented quartz crystals. This layer is enriched in phosphates. Brown apatite and hydrous phosphates form thin (1–2 mm) late veinlets that conform to magmatic lamination. Intergrowths of zinnwaldite with brown apatite and small nests of pegmatite with tourmaline are also typical.
6	500–700	Homogeneous, fine-grained (0.1–0.5 mm) granite. Quartz, K-feldspar and albite grains are mostly anhedral; both feldspars also occur as short subhedral prisms. Grains of quartz, K-feldspar, mica and topaz are markedly zoned. Rims of large feldspar grains have been leached in many places and replaced by late quartz, albite and topaz. Zinnwaldite forms subhedral flakes. Topaz (up to 0.5 mm) is subhedral to euhedral, but small grains (about 0.1 mm) are interstitial. Phosphates—green apatite, amblygonite and childrenite—are the most common accessory minerals.
7	10	Laminated fine-grained layer of granite (similar to layer 1) is present at the base of the dyke with thin veinlets that have intruded into the underlying stock granite.

3.2.2. Early breccia

Early breccia in an isolated block at the south-western contact of the stock consists of fragments of phyllite (diameter <5 cm) cemented with fine-grained

granitic matrix. Some of the fragments are rounded; others are not. Composition of the matrix is similar to that of the stock granite (protolithionite as the dark mica), but it is very fine-grained. Columnar K-feldspars have often grown perpendicular to the surface of the phyllite fragments. Topaz, often present as fragments of older zoned crystals, and apatite are the accessory minerals.

3.2.3. Unidirectional solidification textures

USTs have been developed both in the stock and the dyke granites. Within the stock granite, a UST is found several metres above the major dyke. It is composed of a fine-grained, 1.5-cm-thick quartz layer accompanied by a 3-cm-thick layer of downward-oriented columns of orthoclase (Breiter, 2002). The

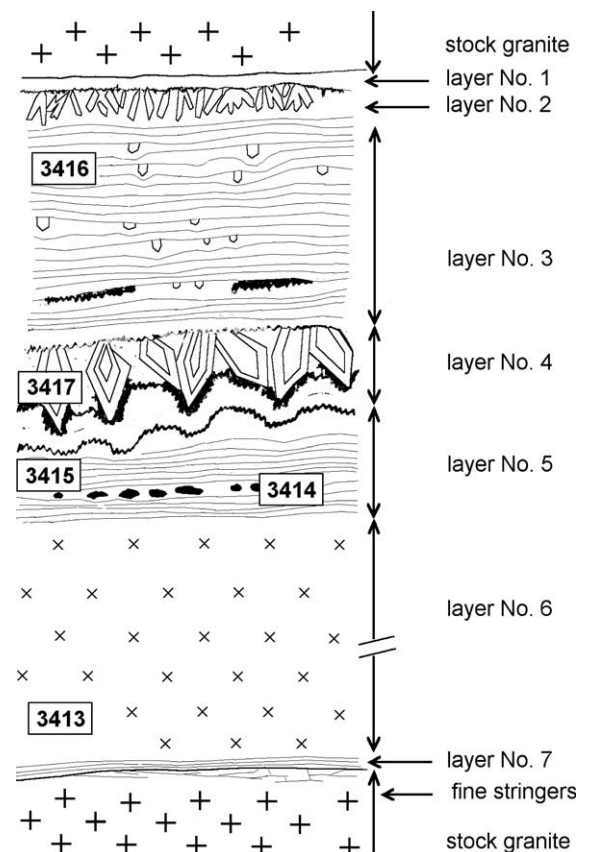


Fig. 3. Schematic vertical section through the western (proximal) part of the major dyke within the quarry (individual layers not to scale). Chemical composition in Table 1, petrographic description in Table 2.

stock granite immediately above and below the UST layer is medium-grained and chemically identical to the stock granite.

USTs occur prominently in the upper part of the major dyke. The western, proximal part of the dyke is exposed across an area of 25 m by 7 to 9 m and consists of seven different layers (Table 2; Figs. 3–5). Mineralogical and chemical composition and grain size of individual laminae in the thinly laminated layers of the dyke (Layers No. 3 and No. 5 in Table 2) differ significantly (Table 3). Boundaries between laminae are commonly sharp (Fig. 6A), but in places diffuse. The newly crystallized fine-grained layers were not entirely solid when the interstitial melt was still present. As a consequence, individual layers were ptygmatically deformed (Fig. 5). Layers of fine-grained zinnwaldite are often overgrown on large comb orthoclase crystals (Fig. 2B). Centimetre-scale intrusions of residual melt into the older layers have also occurred (Fig. 6B).

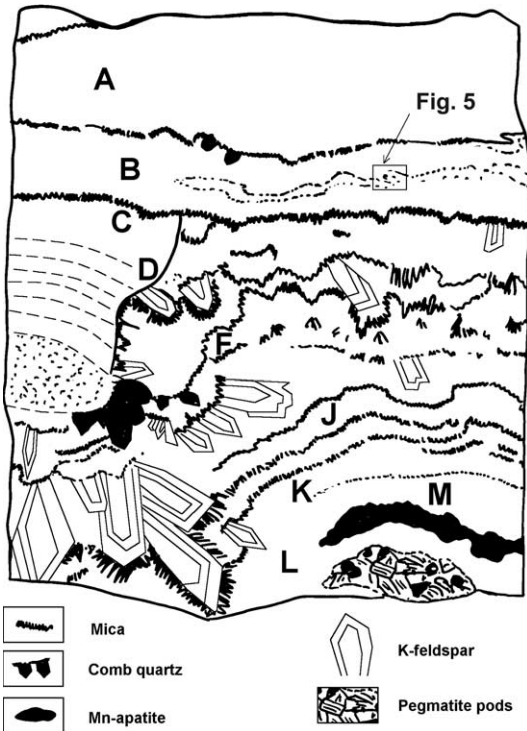


Fig. 4. Detailed structure of the UST in the upper part of the major dyke (natural size 15×13 cm). A through M: location of analysed domains (cf. Table 3). The upper contact of the dyke is 15 cm upwards from the upper margin of the picture.

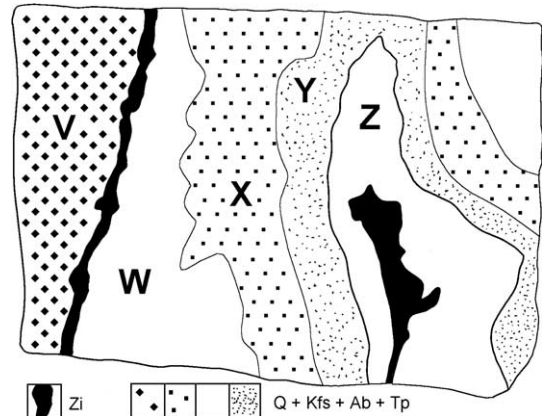


Fig. 5. Detail of the laminated part of the major dyke from Fig. 4. V through Z: location of analysed domains (Table 3). The size of the area described is 2.5×3.5 cm.

3.2.4. Intra-dyke brecciation

The eastern, distal part of the major dyke is not well exposed and a vertical section cannot be

Table 3

Contents of selected elements in the UST layer and laminated domains and brecciated domains of the major dyke at Podlesí

Domain	Laminated dyke in the quarry (Layer No. 3)								
	A	B	C	D	F	J	K	L	M
SiO ₂	68.4	71.0	71.2	68.2	68.7	65.7	67.5	71.4	75.8
Al ₂ O ₃	15.2	13.9	15.7	18.4	15.6	16.5	16.7	11.7	10.4
FeO	0.6	0.5	0.3	0.0	1.1	4.1	1.1	0.8	1.0
CaO	<0.1	0.1	0.1	<0.1	0.2	<0.1	1.5	3.0	0.3
Na ₂ O	5.1	4.8	5.5	7.2	6.5	3.2	1.0	0.6	3.1
K ₂ O	4.5	4.1	1.7	0.7	2.3	5.1	5.3	4.4	3.4
P ₂ O ₅	1.0	0.7	0.5	0.5	0.6	0.3	1.8	3.2	0.9

Domain	Laminated dyke (Layer No. 3), detail					Intra-dyke breccia			
	V	W	X	Y	Z	B1	B2	B3	B4
SiO ₂	74.2	67.5	67.8	65.5	66.1	66.7	69.0	68.7	67.7
Al ₂ O ₃	12.4	16.9	16.5	15.8	17.5	18.5	15.9	17.2	16.5
FeO	0.4	0.1	0.6	0.2	0.2	2.2	1.6	0.4	0.4
CaO	<0.1	0.1	<0.1	<0.1	<0.1	<0.1	<0.1	0.1	<0.1
Na ₂ O	4.9	8.0	6.6	1.6	7.3	3.4	3.8	4.9	6.4
K ₂ O	2.9	1.7	2.9	10.8	3.0	3.4	4.6	2.9	3.4
P ₂ O ₅	0.4	0.7	0.6	1.1	1.0	0.8	0.2	0.8	0.6

Contents (in wt.%) determined at the Czech Geological Survey using defocused electron microprobe analysis (energy-dispersive mode). All analyses are normalised to 95% total oxides (5% reserved for F, Li, Rb and other elements not determined). For location of samples A through M, see Fig. 4; for V through Z, Fig. 5 and for samples B1 through B4, Fig. 7.

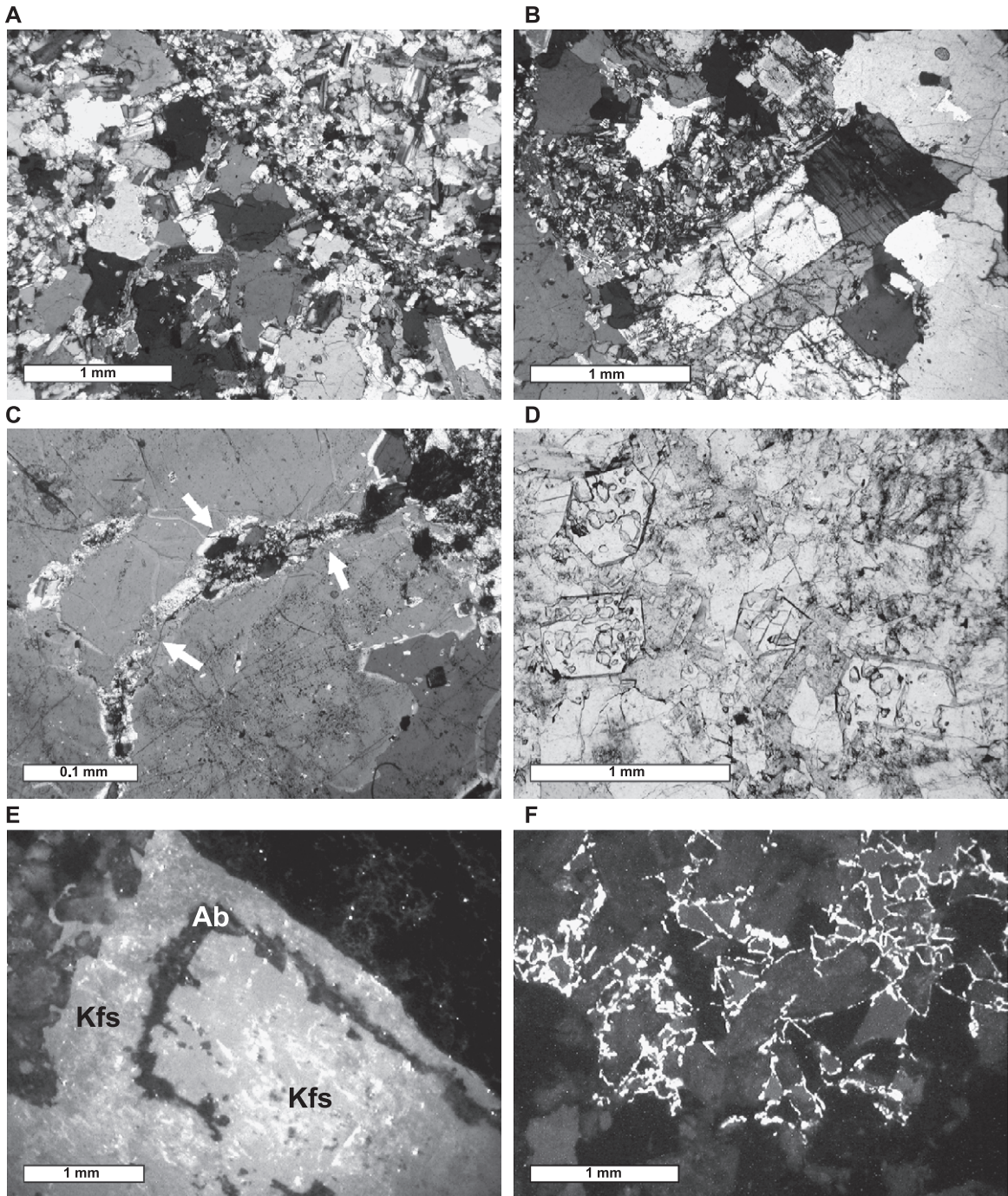


Fig. 6. Photomicrographs of textures in the Podlesi stock. (A) Contact between fine- and very fine-grained laminae in the dyke granite. (B) Invasion of dyke melt into stock granite. (C) Veinlet of late melt in a fractured quartz phenocryst. (D) Topaz from the stock granite with inclusions of quartz. (E) Zone of albite (Ab) in K-feldspar crystal (Kfs) from UST in the brecciated part of the major dyke. (F) CL image of late amblygonite upon feldspar grains in the brecciated dyke.

reconstructed with certainty. The lower part of the dyke consists of layers similar to those described above. The upper part of the dyke consists of 1-mm to 10-cm-thick layers of mica-rich facies (quartz+zinnwaldite+albite+topaz) alternating with layers of mica-poor facies (quartz+albite+K-feldspar>topaz>zinnwaldite). Some of the mica-rich layers are rimmed with a zinnwaldite-dominated UST layer on their footwall. Below this laminated sequence, a 0.5-m-thick layer of magmatic breccia is present (Figs. 2C and 7). Clasts of this breccia are composed of mica-rich facies (fragments of mica-rich layers) and are all around rimmed by zinnwaldite-rich UST (Fig. 8A). The space between the fragments is filled with at least two types of mica-poor matrix, differing in grain size and quartz–albite ratio.

3.2.5. Late cracks in quartz crystals

Quartz and K-feldspar phenocrysts near the upper contact in the proximal part of the major dyke are cracked and the cracks have been filled with fine veinlets of residual melt (Fig. 6C). At least two different types of veinlets are recognised, one Na+F-rich (Q+Ab+Tp) and the other K+P-rich (Kfs+Ap). This fits well the two types of melt inclusions in quartz in the dyke granite (Breiter et al., 1997).

3.3. Mineralogical evidence for magmatic evolution

3.3.1. Alkali feldspars

Alkali feldspars are represented by nearly pure end members—albite (<3% An) and K-feldspar (<5% Ab)—and are rich in P (Frýda and Breiter, 1995; Breiter et al., 2002). The K-feldspars are more significant from a genetic point of view and will be described in detail. The following textural types can be distinguished:

Kfs1 is represented by phenocrysts with perthitic cores and homogeneous rims and contains 0.15% to 0.20% Rb and about 0.4% P₂O₅. It is common in the stock granite. Scarce phenocrysts from the dyke granite reflect a more complicated history: perthitic cores are covered by zones rich in entrapped albite crystals and later rimmed by zones of pure P-rich K-feldspar (Fig. 8B). Such phenocrysts exhibit very bright blue to white colour in cathodoluminescence (CL).

Kfs2, non-perthitic groundmass K-feldspar, is the most abundant type. Larger grains are subhedral, late small grains are anhedral and interstitial. Kfs2 from the stock granite is homogeneous (0.3–0.7% P₂O₅, 0.15–0.25% Rb) and exhibits very bright blue to white CL, whereas Kfs2 from the dyke granite is zoned with P-enriched rims (0.6–1.75% P₂O₅, 0.35–0.5% Rb). In CL, the core is white to bright yellow and the rim

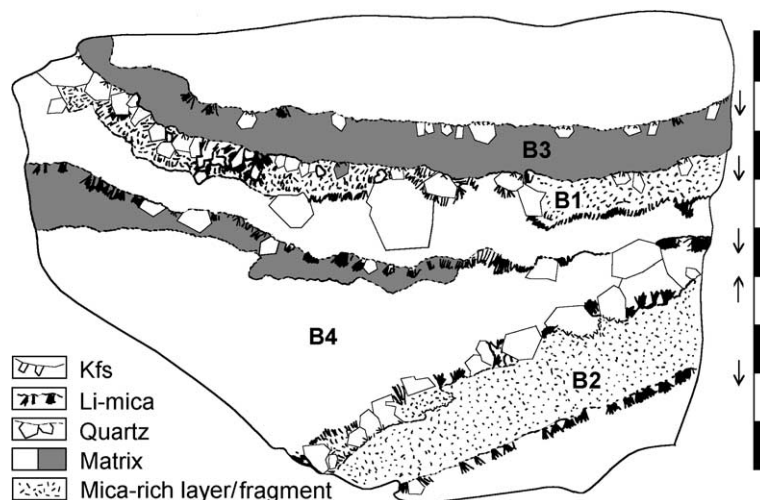


Fig. 7. Detailed structure of the eastern, brecciated part of the major dyke. B1 through B4: location of analysed samples (Table 3). Direction of UST-growth is marked by arrows. Kfs denotes K-feldspar. Scale bar is 9 cm long.

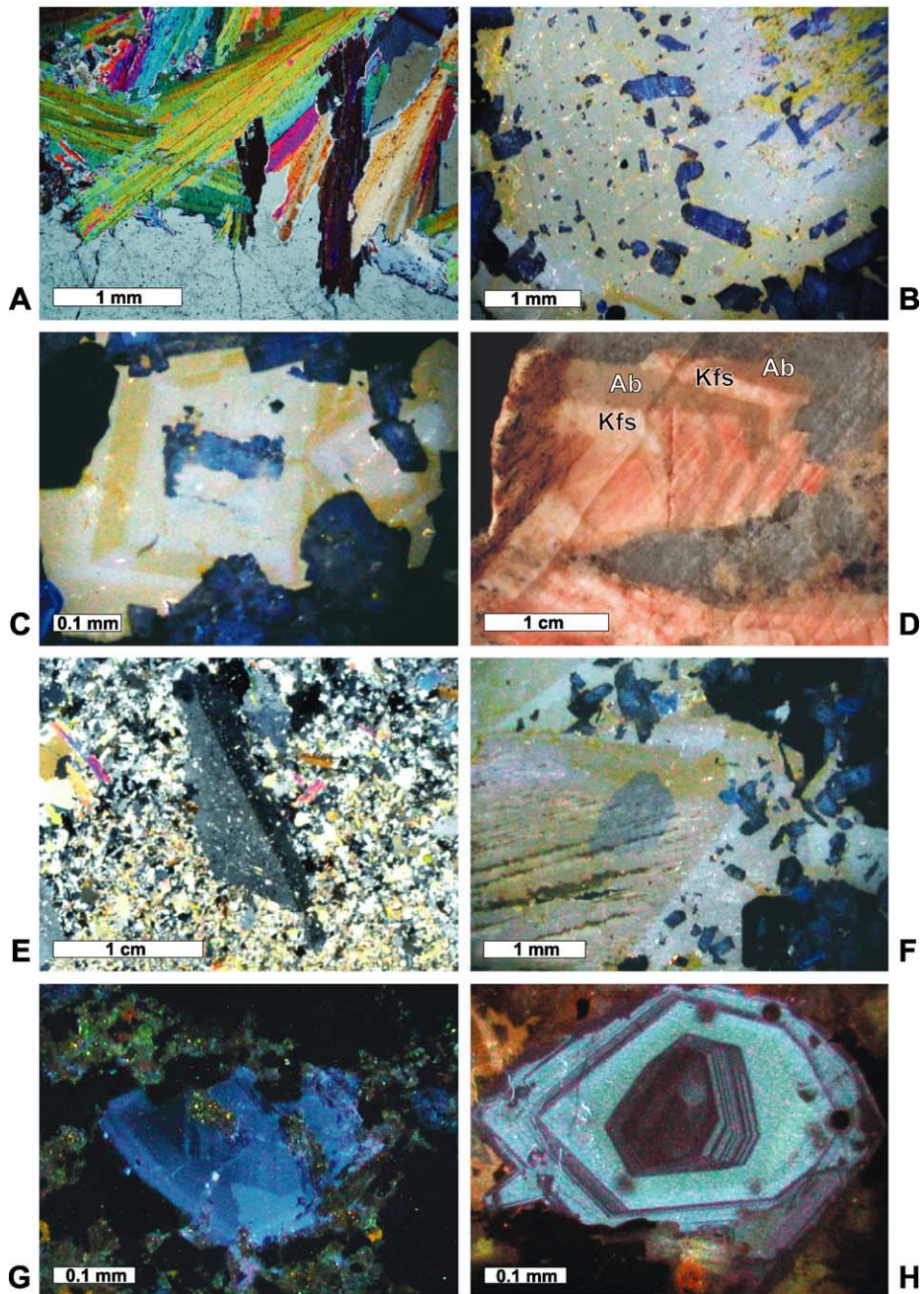


Fig. 8. Photomicrographs of mineral textures from the Podlesí stock. (A) Zinnwaldite-dominated UST from the dyke breccia (crossed polars). (B) CL image of K-feldspar phenocryst (yellow) with perthitic core and abundant albite inclusions (blue) around the core. (C) CL image of zoned matrix K-feldspar from the dyke granite, the dark yellow zones are richest in P. (D) Growth zones of albite in microcline crystal (Kfs) from the stockscheider; (E) Comb orthoclase with zonally arranged albite inclusions (crossed polars). (F) CL image of a comb K-feldspar crystal from the brecciated dyke—the core is perthitic (dark yellow) and the P-rich rim (light yellow) contains euhedral albite inclusions (blue). (G) CL image of fragmented and/or altered topaz crystal from the explosive breccia. (H) CL image of late topaz from the dyke granite.

yellow to brownish (Fig. 8C). In the laminated part of the major dyke, the content of Rb in Kfs2 reaches 0.7%.

Kfs3 forms large crystals that have grown perpendicular to the contact in the stockscheider. The inner parts of the crystals are moderately enriched in P (0.6–0.8% P_2O_5); the outer zones have been partially leached and depleted in P (0.1–0.3% P_2O_5) and contain small inclusions of apatite visible in the CL images. Of all the K-feldspar types, only Kfs3 is triclinic. It exhibits a very bright blue to white colour in CL. A remarkable feature of some feldspar megacrysts is the appearance of albitic growth zones inside the microcline crystals (Fig. 8D). Microclines in the brecciated stockscheider are altered, P-free and do not exhibit any CL.

Kfs4 is represented by large crystals from the UST layer of the dyke granite. These crystals typically have macroscopically visible zones with dominant pale cores upon which thin (up to 2 mm) colourless rims have crystallized. Microscopically, the cores contain numerous inclusions of small albite crystals oriented parallel to the growth zones of K-feldspar, the rims contain only scarce albite inclusions (Fig. 8E). No apatite occurs within the Kfs4 crystals. Distribution of P (0.6–0.9% P_2O_5) and Rb (0.3–0.4% Rb) is homogeneous, sometimes with slight enrichment in the rims. The content of P in the albite inclusions is also very homogeneous and only slightly lower than in K-feldspar (Fig. 9). Comb K-feldspar in the

brecciated part of the dyke is less abundant and forms up to 5-mm-long prismatic crystals, slightly zoned in CL. Some crystals have a perthitic core and clusters of Ab-inclusions in the outer zone (Fig. 8F), others have a homogeneous core and a rim divided by an albite zone (Fig. 6D). Both of these subtypes of Kfs4 are rich in P.

Albite is found in the granite types only in the groundmass. The P content in albite is generally lower and more uniform than in K-feldspar, typically between 0.05 and 0.7 wt.% P_2O_5 in the stock granite. Albite from the dyke granite contains 0.2–1.0 wt.% P_2O_5 . This albite is zoned but the zoning is weaker than in the K-feldspar. In perthite, the admixed albite is usually depleted in P relative to the surrounding K-feldspar. In CL, albite exhibits a poorly developed zoning and medium to dark blue colours.

3.3.2. Quartz

Quartz was studied in detail by Müller et al. (2002). Based on CL and textural studies five magmatic quartz populations can be distinguished. The stock granite contains rare euhedral quartz phenocrysts (Q1, 1–5 mm) that show complex growth zoning. A red-brown luminescent core is overgrown by blue luminescent oscillatory growth zones. Marginally, the phenocrysts are strongly embayed. The zoning parallels the shape of lobate embayments (Fig. 10a). The phenocrysts are overgrown by anhedral fine-grained groundmass quartz (Q2) which

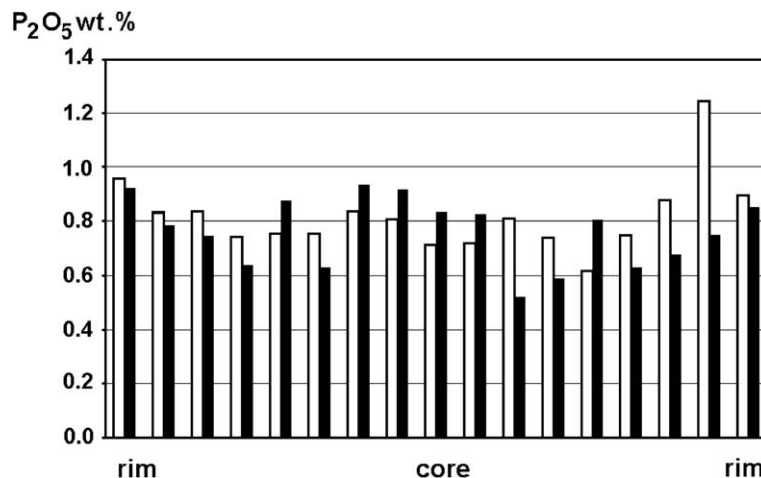


Fig. 9. Distribution of P in comb orthoclase (white columns) with albite inclusions (black columns) from the proximal dyke (cf. Fig. 8E). At each point, albite inclusion and adjacent orthoclase were analysed. Distance between the individual points is about 0.1 mm.

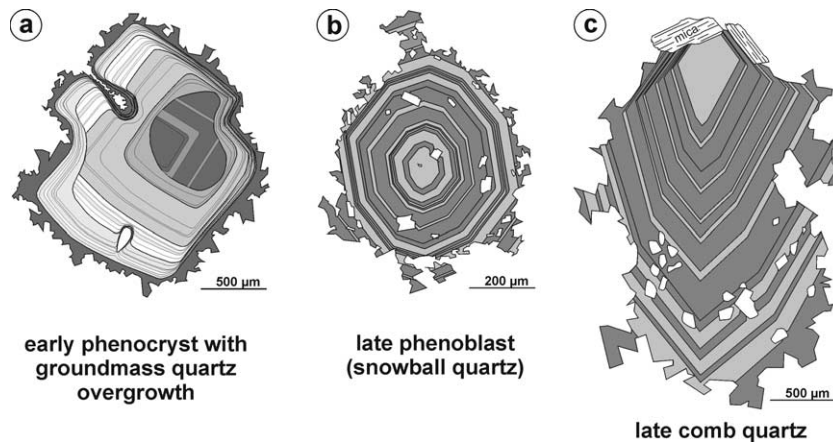


Fig. 10. Growth patterns in quartz: (a) phenocryst (Q1) with groundmass quartz overgrowth (Q2); (b) snowball quartz (Q3); (c) comb quartz (Q5). (a) and (b) modified from Müller et al. (2002).

is free of growth zoning and shows weak red-brown CL. Secondary structures are characterized by bright halos around radioactive micro-inclusions and non-luminescent, neocrystallized domains. Like groundmass quartz, stockscheider quartz (Q3) is free of growth zoning, shows red-brown luminescence, and contains a number of secondary structures.

In the dyke, the quartz forms snowball-textured phenoblasts (Q4) 0.2 to 1.5 mm in size. Generally, the snowball quartz has a red- to red-brown CL and shows continuous growth into the matrix quartz, recognisable by the ramified, amoebic grain boundaries, and penetrates the matrix. The crystals commonly contain inclusions of the groundmass minerals. Furthermore, in many cases fluid and melt inclusions are present. Numerous tabular albite crystals envelope the phenoblast edge indicating that the quartz did not incorporate albite as it grew. The phenoblasts show oscillatory growth zoning characterized by planar bordered growth zones with α -quartz habit, which continues into the amoebic crystal margin and into the matrix quartz without any changes in the CL properties (Fig. 10b). Comb quartz (Q5) nucleated in the fan-like zinnwaldite layers of UST exhibits growth patterns and CL colours similar to snowball quartz (Fig. 10c).

A late- to post-magmatic fluid-driven overprint (e.g., micro-fracturing and greisenisation) has caused small-scale dissolution, precipitation and re-equilibration of pre-existing quartz (Q1–5) along grain boundaries, intra-granular micro-cracks, and around

fluid inclusions. This neocrystallized quartz (Q6) may be of different generations not distinguishable by the methods used in this study.

In order to better understand the crystallization conditions of the different quartz types, contents of the trace elements Ti, Al, K and Fe were determined by Müller et al. (2002). The plot of Al and Ti contents in the magmatic quartz populations (1 through 5) yields a trend reflecting the evolution of the magma (Fig. 11). The early crystallization stage represented by the quartz phenocrysts is characterized by high Ti and low Al concentrations in the quartz lattice. During further evolution Ti decreases whereas Al increases. The post-magmatic neocrystallized quartz of the healing structures is outside the magmatic trend (for details, see Müller et al., 2002).

3.3.3. *Li-rich mica*

Trioctahedral F-rich Li–Fe micas are the only mafic minerals in all the granite types. Their chemical composition differs depending on the host granite type and textural position:

1. The mica in the stock granite is generally homogeneous protolithionite (in the sense of Weiss et al., 1993). In many places, it contains small grains of radioactive minerals with pleochroic haloes. F contents reach 5 to 7 wt.%, Li_2O 2.0 to 2.5 wt.%, Rb 0.8 to 1.0 wt.% and Cs 0.2 wt.%.

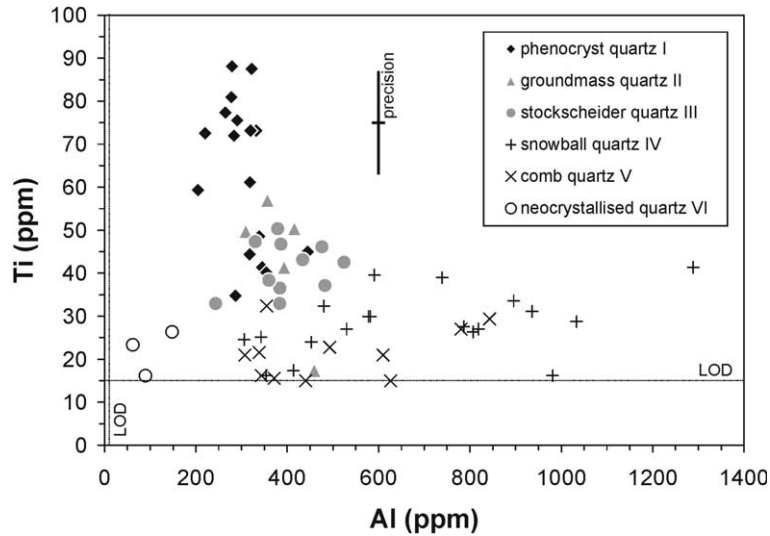


Fig. 11. Plot of Ti versus Al concentrations in the different quartz populations (I through VI—see text for more details). LOD indicates limit of detection. Modified from Müller et al. (2002).

2. The dyke granite contains a distinctly zoned zinnwaldite in the groundmass with cores relatively enriched in Fe, Mg and Ti, and rims higher in Si and Li. There is no zoning in the F, Rb and Cs contents. Compared with protolithionite, zinnwaldite is enriched in F (6–8 wt.%), Li_2O (3.5–4.7 wt.%) and Rb (1.0–1.1 wt.%), but depleted in Cs (about 0.1 wt.%).
3. Fan-like UST aggregates of zinnwaldite (Fig. 8A) occur within the brecciated parts of the dyke. Zinnwaldite is the oldest mineral within the zinnwaldite-rich sections of UST and the crystals often extend into older quartz–feldspar laminae. In K-feldspar rich sections, zinnwaldite borders comb feldspar. The UST zinnwaldite contains 7.5 to 7.7 wt.% F, 4.5 to 4.6 wt.% Li_2O , 1.2 to 1.3 wt.% Rb and about 0.1 wt.% Cs. Zoning of the UST-zinnwaldite in the dyke breccia is the opposite compared to the zinnwaldite in the groundmass: the roots are Fe-poor, the terminal parts of aggregates are relatively Fe- and locally also Mg- and Ti-enriched.

Hydrothermal F-rich Li-biotite (<1 wt.% Li_2O) is common in greisen stringers. Muscovite was found only as a rare product of hydrothermal alteration in the stockscheider and near the greisen stringers.

3.3.4. Topaz

Topaz is present in two types. Euhedral to subhedral crystals with intensive oscillatory CL-zoning (Tp1) are found in all the rock types. This type contains numerous irregular inclusions of quartz (Fig. 6E). Fragments of crushed and altered zoned topaz crystals are present in the matrix of the early breccia (Fig. 8G). Tp1 forms, together with the QI, the earliest crystallized minerals. Late, interstitial topaz crystals (Tp2) occur only in the dyke granite and exhibit intensive blue CL-zoning (Fig. 8H). Both types of topaz are rich in F (90–97% of theoretical F-saturation), the late topaz is also rich in phosphorus (up to 1 wt.% of P_2O_5 ; Breiter and Kronz, 2003).

3.3.5. Phosphates

Two generations of fluorapatite are present: early Mn-poor euhedral green crystals and later Mn-rich interstitial flakes. Brown variety of late Mn-rich apatite forms small nests and aggregates with zinnwaldite in a laminated zone immediately below the UST layer. All types are poor in Cl (mostly below 0.1 wt.% Cl) and exhibit intensive yellow CL. Small prismatic crystals of childrenite–eosphorite, amblygonite and zwiesselite, and irregular grains of triphylite are found in the dyke granite (Breiter, 2002). Their texture suggests a relatively late, yet

magmatic origin. Thin layers of late amblygonite on the feldspar grains (Fig. 6F) and small grains (up to 1 mm²) of hydrated phosphates of Al, Ca, Fe and Mn are also found in the dyke granite.

4. Discussion

4.1. F, P, B and H₂O saturation

The Podlesí stock is rich in F: the stock granite contains 0.6 to 1.8 wt.% F, the dyke granite 1.4 to 2.4 wt.% and the intra-dyke breccia up to 3.8 wt.%. A high content of F in magmatic amblygonite (9.4–10.3 wt.%) reflects, according to London et al. (2001), 2.5 to 3.0 wt.% of F in the crystallized melts. This is consistent also with the F contents in zinnwaldite and topaz, which are greater than 90% of the theoretical maxima.

P was already enriched in the parental stock granite melt (0.5% P₂O₅). High peraluminosity coupled with low Ca content suppressed nucleation of apatite and promoted further enrichment of P (about 1 wt.% P₂O₅) in the dyke granite melt. London et al. (1993) calibrated the ratio between alkali feldspar and coexisting melt as $D_P^{Afs/melt} = 2.05ASI - 1.75$ and $D_P^{Or/Ab} = 1.2$. Also, according to the P content in the rims of K-feldspars in the dyke groundmass, the maximum P content of the crystallized melt reached about 2 wt.% in restricted domains. Although the substitution of P in the feldspars is coupled with Al, any other component that decreases the activity of Al, F for instance, will also decrease the partition coefficient. Thus in the fragments of the intra-dyke breccia, the most F-rich and P-rich domains of the dyke (3.8 wt.% F, 1.3 wt.% P₂O₅), the P content in K-feldspars is relatively low (~1 wt.%).

The B content in the granites is negligible (20–60 ppm), but an extensive outer contact aureole of tourmalinisation in the phyllite several hundreds of metres thick indicates that a large amount of B emanated from the crystallized magma. Tourmaline is found along numerous fractures in phyllite, locally along the foliation in the whole rock, ultimately changing the chlorite–sericite phyllite into quartz–tourmaline rock with up to 0.5 wt.% B. Crystallization of tourmaline from granitic melt in equilibrium with Fe–mica in relevant conditions (500–600 °C, 1 kbar)

requires about 2 wt.% of B in the melt and a high content of F requires even higher contents of B at this equilibrium (Wolf and London, 1997). Because no primary magmatic tourmaline is found in the granite, the primary B content in the melt probably did not exceed 2–2.5 wt.%. The only exceptions are the small pockets (<4 mm in diameter) within the UST layers filled by tourmaline (schorl). Here, droplets of residual liquids were likely enriched in B up to the stability field of tourmaline.

It is difficult to estimate the water content in the Podlesí granite melt, but some constraints are available: the primary melt should have been water-undersaturated during emplacement as a water-saturated melt would have rapidly crystallized at decreasing pressure (Johannes and Holz, 1996; Sykes and Holloway, 1987). Forceful early brecciation followed by extensive fluid escape shows that the melt became water-saturated shortly after emplacement. As deduced from the composition of mica, feldspars and topaz, the dyke granite melt was relatively rich in F, P, Li and Al—all these elements enhance the water solubility and lower the solidus (Johannes and Holz, 1996). Thus, the dyke granite magma was probably also undersaturated. Crystallization of the assemblage quartz–K-feldspar–albite–zinnwaldite–topaz enhanced the water content of melt (as the OH/F sites in mica and topaz were saturated with F). Breiter et al. (1997) determined 7 eq.-wt.% water from melt inclusions in the dyke granite quartz, but it is not clear whether this melt was water-saturated. From the melt inclusions in the stockscheider in Ehrenfriedersdorf (comparable to Podlesí), Thomas et al. (2003) deduced a full transition from B-rich silicate melt to B-rich water-based vapour. Thus, no water-saturation limit seems to exist in such a specialised melt. In the Podlesí dyke granite, the presence of late brecciation suggests that water saturation was reached.

4.2. Magmatic brecciation

Most ore-related breccias described from granitic bodies are related to late magmatic-hydrothermal stages of porphyry-type intrusion (Sillitoe, 1985). These breccias (their roots), which typically occur inside the plutons, were formed by aqueous fluid and cemented by hydrothermal quartz, chlorite, etc. Less abundant are early magmatic breccias in which the

fragments are cemented by the rapidly cooled granitic melt. Small intrusions of tin-bearing granites in Krušné Hory/Erzgebirge contain related pipes of early magmatic breccias as a typical constituent (Oelsner, 1952; Schust and Wasternack, 1972; Seltnann and Schilka, 1991; Jarchovský and Pavlů, 1991). This type of breccia typically occurs at the top of the granite intrusions and is composed of country rock fragments cemented by rapidly cooled granitic melt and greisenised. In some cases, several episodes of brecciation may be superimposed in the same pipe (Gottesberg: Gottesmann et al., 1994; Sadisdorf: Seltnann, 1994).

In Podlesí, the top of the intrusion with supposed breccia pipe has already been removed. Extensive fracturing of the phyllite envelope, presence of an isolated block of phyllite breccia and brecciated stockscheider, and an overall similarity with explosive breccias described by Seltnann and Schilka (1991) support our interpretation of the early breccia from Podlesí as a forceful explosive event. Microclinalisation of K-feldspars, loss of Li from mica and alteration of topaz in stockscheider indicates intensive reaction with fluid. Thus, the probable timing of the early brecciation was during the crystallization of the stockscheider. Escape of hydrous fluids during the early brecciation was probably also responsible for B loss from the magma, which led to tourmalinisation of the outer contact aureole. The later intra-dyke breccia from Podlesí, although situated within the granite body, should be also assigned to the class of “early breccias” according to Sillitoe (1985), as it is cemented by granite matrix without visible influence of hydrothermal fluids.

Another possible mechanism for brecciation and opening of the Podlesí system could have been an input of external water into the crystallizing magma (Bardintzeff, 1999). Oxygen isotope data, however, do not favour influence of meteoritic water (Žák et al., 2001).

4.3. Zoned crystals

The different populations and zoning of quartz, K-feldspar, micas and topaz reflect several stages of crystallization history of the rocks. Sharp boundaries between the zones and zones of partial resorption indicate rapid and substantial changes in the p - T - X

conditions of the magma. The zoning of feldspars and mica grains in the dyke granite imply two major stages in the crystallization history of this rock, whereas only one major crystallization stage can be deduced for the stock granite. The unzoned, mostly perthitic K-feldspar and unzoned mica crystals of the stock granite are nearly identical to the K-feldspar and mica cores in the dyke granite and represent an older crystallization stage from the melt. In contrast, the P-enriched rims of K-feldspar and Li-enriched rims of mica in the dyke granite document a distinctly more evolved environment enriched in P and F. The inherited cores of K-feldspar and mica crystals in the dyke granite indicate that the magma intruded into flat joints was a mixture of melt and entrapped crystals.

Another style of K-feldspar zoning is developed in the UST layer. The comb orthoclase is rich in albite inclusions and has inclusion-poor rims with sharp borders between the two domains. This points to abrupt changes in crystallization conditions. The early growth of K-feldspar crystals promoted local saturation of incompatible constituents in the boundary layer. This resulted in the crystallization of zonally arranged albite crystals in the inner parts of comb K-feldspar (Fig. 8B) and snowball quartz (Fig. 10b). Later, the rims crystallized in conditions that allowed Na to diffuse away and contribute to the growth albite crystals in the matrix.

The contents of P_2O_5 in albite inclusions and adjacent K-feldspar (Fig. 9) fit with experimental observation (London et al., 1993) that implies a $D_P^{Or/Ab}=1.2$. This supports magmatic origin for the comb feldspars via crystallization from silicate melt without later re-equilibration. Lamellae of albite inside the microcline crystals within the stockscheider (Fig. 8B) are similar to crystals obtained by Petersen and Lofgren (1986) during eutectic experiments. According to Petersen and Lofgren (1986), these intergrowths may be explained as a product of boundary layer crystallization from an undercooled melt.

Because the Podlesí system is rich in P, it might be expected that P would have entered the lattice of quartz according to the berlinite substitution $P^{5+}+Al^{3+}=Si^{4+}+Si^4$ (e.g., Maschmeyer and Lehmann, 1983). Larsen et al. (2002; personal communication, 2002) reported P and Al contents of about 40 and 175

ppm, respectively, in pegmatitic quartz in south Norway. Quartz from Podlesí, although Al-rich, contains less than 60 ppm P (the detection limit of the electron microprobe).

4.4. *Stockscheider and K-feldspar-dominated UST layers in the dyke*

Both the stockscheider and the K-feldspar-dominated UST layer are similar in that they contain large oriented K-feldspar crystals together with quartz and a fine-grained granitic matrix. However, the whole-rock chemical composition, internal fabric and composition of quartz and K-feldspar of these rock types differ significantly. The Ti content in the stockscheider quartz is twice as high as that in the comb quartz, whereas Al is much more enriched in the comb quartz (Fig. 11). This illustrates the course of magmatic evolution from the early crystallization of stockscheider at the top of the intrusion to the late crystallization of UST layers within the dyke.

The bulk composition of the stockscheider (3361 in Table 1) is similar to the bulk composition of the stock granite. This means that crystallization of the large K-feldspar crystals in the stockscheider was complemented by crystallization of the quartz–albite matrix with no substantial addition of K. The bulk composition of the K-feldspar-dominated UST layer (3417 in Table 1) is markedly different from the bulk composition of the dyke granite—it is strongly enriched in K and Al and depleted in Si and Na. The bulk composition of the UST layer can be modelled as a mixture of the dyke-granite melt with 25% K-feldspar added. According to London (1999), the growth of comb K-feldspar crystals may be explained by crystallization in the boundary layer, which effectively removed K from the adjacent melt. Such preferential consumption of K would be expected to deplete K in the melt from which the adjacent fine-grained layer was crystallized. This is true for the stockscheider but not for the UST.

4.5. *Magmatic layering and UST*

Simple magmatic layering with non-oriented crystals or with orientation of minerals parallel to the layers is common in aplite–pegmatite bodies (Breaks and Moore, 1992; Morgan and London, 1999). A

well-known example of magmatic layering is the B-rich Calamity Peak granite–pegmatite complex in South Dakota, USA, which includes a 400-m-thick series of alternating pegmatite and layered aplite, in 0.1- to 2-m-thick layers (Rockhold et al., 1987). Magmatic layering in B-poor granites is much less frequently reported. When present, it has crystallized inward from the outer contacts (Baluj, 1995; Zraisky et al., 1997; Frindt, 2002). Magmatic layering with crystals oriented perpendicular to the individual layers (UST) is typically found in subvolcanic granitic stocks associated with Mo and/or W±Sn mineralisation. Layering is typically parallel to the contact and is expressed by alternating layers of euhedral comb quartz crystals and fine-grained aplite (Kormilicyn and Manujlova, 1957; Shannon et al., 1982; Kirkham and Sinclair, 1988). K-feldspar UST and also rare tourmaline UST have been described from aplite–pegmatites (Duke et al., 1992; London, 1992).

In layered granites, the bulk composition of layered domains is similar to the bulk composition of the whole body (Zraisky et al., 1997). The layered aplite–pegmatites are commonly differentiated into a slightly Na-enriched lower aplite and K-enriched upper pegmatite (Duke et al., 1992; Morgan and London, 1999). The oldest model for layering and UST in aplite–pegmatites involved preferential partitioning of Na into lower aplite and K into aqueous fluid that precipitated as the upper pegmatite (Jahns and Tuttle, 1963; Jahns and Burnham, 1969). This model was later discredited and replaced by models based on the undercooling of H₂O-rich melt (see overview in London, 1992, 1996). Fenn (1977) stated that the nucleation density of feldspar fell sharply with increasing H₂O, which resulted in the growth of large crystals from the H₂O-saturated melt. At the same degree of undercooling, the nucleation density of alkali feldspars is suppressed much more than that of quartz (London et al., 1989), so the K-feldspar grains grow larger than the associated quartz grains. Also Webber et al. (1997) stressed the significance of undercooling for heterogeneous nucleation and oscillatory crystal growth. London (1999), after experiments with B, F and P-doped granitic melt, preferred the boundary-layer effect in undercooled melt (>100 °C below the liquidus) as the cause for the layered textures.

Part of the problem of all the models based on undercooling is how to explain repetitive UST layers. For this, repetitive episodes of “undercooling” (=crystallization of UST layer) and “warming” minimally up to eutectic temperature (=crystallization of aplitic or granitic layers) will be necessary. Such fluctuation inside a relatively thin dyke cannot be explained via cooling at a constant pressure. Alternatively, a sudden adiabatic drop of pressure during opening of the system causing “undercooling” could have been followed by a pressure increase, restoring the conditions of “standard” granitic crystallization (Fig. 12). This model fits well the observed intra-dyke brecciation.

Oscillation of fluid pressure due to episodic degassing is also the basis for the “swinging eutectic” model (term coined by D. Jahns in 1982). Changes in pressure resulted in expansion of either the quartz field at high pressure or the albite field at low pressure and further crystallization of albite–quartz line rock (Balashov et al., 2000). Fedkin et al. (2002) made experiments with P- and F-doped granite from Podlesí and obtained a glass specimen with thin bands differing in the contents of Al, Si, F, P and alkalis.

Cox et al. (1996) showed that the rate of nucleation and size of K-feldspar crystals depend on the water content of a granitic melt. Depletion in water lowered the nucleation rate and promoted the formation of large K-feldspar crystals. Thus, the presence of large K-feldspar crystals in the UST layers in Podlesí may indicate water deficiency.

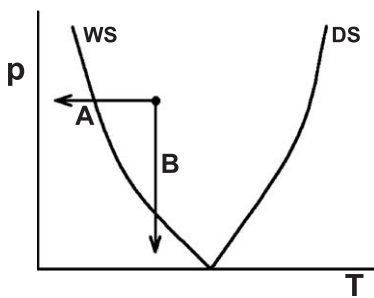


Fig. 12. Diagram indicating possible ways to produce repeated UST layers. A—cooling path at constant pressure; this process is irreversible without an additional heat source. B—adiabatic cooling path of water-rich melt after opening of the system. Later, when the joints are filled with crystallizing melt, the pressure increases again. This process is almost reversible and may produce repeated UST layers. WS—solidus of wet melt, DS—solidus of dry melt.

The UST domains in porphyry-type systems may contain >60% of modal quartz and thus these layers are not consistent with the overall granitic composition of the parental porphyry melt. The strong silica enrichment within the comb layers has been explained by addition of quartz from an aqueous fluid (Kirkham and Sinclair, 1988; Lowenstern and Sinclair, 1996). Recently, Taylor et al. (2002) introduced a model for crystallization of giant quartz crystals via aluminosilicic hydrogel supported by an internal aqueous fluid, while D. London (personal communication, 2003) preferred, also in this case, crystallization from the boundary layer of fluxes-enriched silicate melt.

At Podlesí, UST layers are defined by K-feldspar or zinnwaldite. This mineralogical feature, together with strong enrichment of large-ion lithophile elements (LILE), makes the Podlesí system more comparable to aplite–pegmatite bodies with UST layers than to porphyry type intrusions. Nevertheless, with the exception of the 10-cm-thick K-feldspar-dominated UST, there is no K-enrichment and Na-depletion in the upper part of the dyke. Also the lack of B is an important difference between the Podlesí granites and other layered aplite–pegmatites.

The trigonal habit of the zoning in the snowball quartz, the frequently enclosed groundmass minerals and the occurrence of melt inclusions indicate growth of the snowball quartz in a nearly non-convecting and fluid-saturated crystal mush at <600 °C (<1 kbar). The extrapolated solidus temperature (Breiter et al., 1997) is 610 ± 26 °C for the melt of the dyke granite, which is in agreement with the trigonal habit of the quartz crystals. Although the dyke granite magma was rapidly cooled (undercooled as indicated by the USTs), no classic mineralogical and textural markers of rapid cooling, such as needle-like apatite, glassy spherules or very fine-grained marginal facies (cf. Best and Christiansen, 2001) are present. This reflects the substantial differences in behaviour during rapid cooling between an ordinary granitic magma and a peraluminous magma strongly enriched in water and fluxes.

Individual laminae show a large scatter of normative compositions (Fig. 13), another feature supporting non-eutectic crystallization in an open system. Mica-rich fragments of breccia are shifted towards the Ab–Q join, which may be attributed to high contents of Li and dissolved water in melt (Johannes and Holtz,

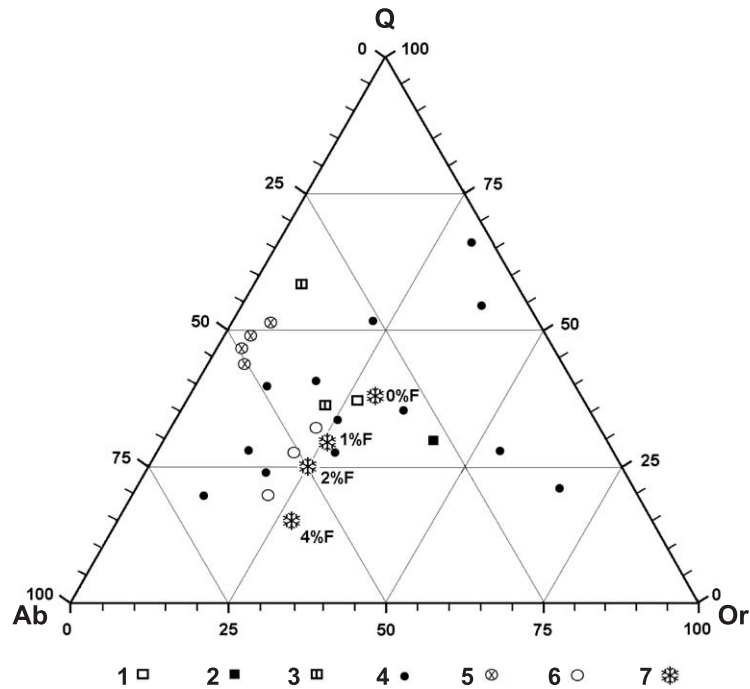


Fig. 13. Normative Ab–Or–Q triangle showing the composition of individual samples in the major dyke of Podlesí. Key to the symbols: 1—laminated rock above the UST layer; 2—UST; 3—laminated rock under the UST layer; 4—individual laminae in laminated rock; 5—fragments in the brecciated dyke; 6—individual laminae in matrix in brecciated dyke; 7—position of the minima for the water-saturated system without F and with 1, 2 and 4 wt.% F added ($p_{\text{H}_2\text{O}}=1$ kbar) (according to Manning, 1981). Modified from Breiter (2002).

1996). The breccia matrix lies near the expected evolutionary path of granitic melt with 2% to 4% F (Manning, 1981). The actual F content in the breccia matrix is lower but, at the time of crystallization, it was probably higher, i.e., more than 3 wt.%. Because of a high melt/water partition coefficient, F did not escape with the fluids during opening of the system. Thus, the matrix, although mica-poor, crystallized topaz-rich.

4.6. Comparison with other P-rich fractionated granites

Rare-metal granites enriched in P are typical for the European Variscan belt. Only a few, however, are comparable to the Podlesí system in the degree of P and F enrichment. In the Beauvoir granite (France), metre-wide zones of layers composed of lepidolite and albite with marked grain size variation are associated mainly with the transitional zones between individual intrusive units. One of these layers is

brecciated and cemented by later injection of magma. The layering was interpreted as the product of magmatic flow (Jacquot, 1987; Cuney et al., 1992). No stockscheider has been found, but the so-called “fringe” zone near its upper contact contains thin layers enriched in lepidolite, albite, columbite and cassiterite (Raimbault et al., 1995).

The P-rich Mesozoic Ta-bearing granite at Yichun (China) consists of a sheet-like body with a huge stockscheider at the top. Vertical changes in K-feldspar/albite ratio are evident but no real stratification was encountered within the flat, 43-m-thick body. The granite was strongly re-equilibrated with hydrothermal fluids, as documented by disturbed P contents between albite inclusions and their snowball-type K-feldspar host, but no indications of opening have been found (Huang et al., 2002).

The mica-rich layer of the distal dyke in Podlesí contains 24% quartz, 33% albite, 34% zinnwaldite, 5% topaz and 4% K-feldspar, which may be transitional between F-rich granites and a group of F-rich

rocks termed “ongonite” (Kovalenko and Kovalenko, 1976), “topazite” (Eadington and Nashar, 1978; Johnston and Chappell, 1992) or “magmatic greisens” (Xiong et al., 1999). The very high F content is manifested by high modal contents of topaz and zinnwaldite and the absence of K-feldspar, because all K is bound in the mica. The F content in the distal dyke is higher than in ongonites and the presence of magmatic albite in Podlesí fragments distinguishes them from topazite. Experiments by Xiong et al. (1999) using albite granite with up to 6% of F produced quartz, topaz and mica together with an alkali-rich fluid at <600 °C. Albite appeared in the crystallized assemblage when F in the system was below 4 wt.% (Xiong et al., 1999). The mica-rich facies from Podlesí substantiates these experiments and stability of albite near solidus up to 4 wt.% of F. Moreover, incorporation of nearly all K into micas inhibited K-feldspar crystallization, which indicates a possible way to produce magmatic mica-rich “greisen”. Thus, the Podlesí system seems to be quite unique in its complexity, including crystallization of stockscheider, early and late brecciation, magmatic layering and UST.

5. Genetic scenario and conclusions

The Podlesí granites were crystallized from fractionated granitic melt progressively enriched in F, P, Li and H₂O. Crystallization conditions changed abruptly as documented by complicated zonation of quartz, feldspars and mica crystals. Stockscheider, magmatic layering and UST give evidence for repeated episodes of nonequilibrium crystallization probably from undercooled melt. Two episodes of magmatic brecciation and extensive escape of B-bearing fluids resulting in tourmalinisation of surrounding phyllite indicate that the system was opened at least twice and exposed to an abrupt decrease of pressure. Mineralogical evidence of post-magmatic, aqueous fluid-related processes is restricted, so we believe that the system has preserved its magmatic condition. Although brecciation has occurred, the Podlesí rocks are more comparable to layered aplite–pegmatites than to porphyry-type intrusions with comb layers. Among the evolutionary models for layering and UST, a combination of undercooling

(Webber et al., 1997; London, 1999) and pressure changes (“swinging eutectic”; Balashov et al., 2000) seems to be the most plausible.

We envisage the following four evolutionary stages for the Podlesí system:

1. Emplacement of the stock granite melt at a shallow level, crystallization of the stockscheider, enrichment of water and fluxes at the top of the magma body, and brecciation of the stockscheider and overlying phyllites, caused by the escape of the exsolved water (first opening of the system) and followed by escape of fluid and tourmalinisation of the phyllites.
2. Fine-grained granitic matrix of the breccia (and the granite) crystallized from a volatile-poor melt and is composed of Li-biotite, P-poor feldspars and homogeneous quartz, all without zoning. Topaz is only an accessory, often in fragments. Beneath this rapidly crystallized “cork”, water and fluxes became again slowly enriched. The stock is generally formed of albite–protolithionite–topaz granite (A/CNK=1.15–1.25, 0.4–0.8 wt.% P₂O₅, 0.6–1.8 wt.% F, 0.15–0.20 wt.% Li). Subsequent crystallization of parental melt produced a small amount of a more F, P, Li- and water-rich residual magma. When the upper part of the stock had crystallized and cooled sufficiently to allow brittle fracturing, this residual magma (A/CNK=1.2–1.4, 0.6–1.5 wt.% P₂O₅, 1.4–2.4 wt.% F, 0.2–0.3 wt.% Li) penetrated upward, forming a set of flat dykes.
3. Crystallization of the major dyke proceeded from the contacts inwards. Crystallization from the bottom proceeded more rapidly and crystallization from the upper contact produced layered rock. When a substantial part of the dyke had crystallized (probably more than 80 vol.%), the rest of the magma become water-oversaturated, the liberated vapour escaped (the second opening) and the pressure dropped. Decrease of pressure caused undercooling and crystallization of the UST. Repetition of UST layers is explained by fluctuation of pressure in nearly adiabatic conditions. Escape of fluids also promoted local intra-dyke brecciation.
4. Cementation of dyke fragments with late magma. Late amblygonite crystallized from P-rich fluid.

During the final consolidation of the deeper parts of the system, F-rich and Li-poor aqueous fluids were released. These fluids, also enriched in Sn and W, ascended along steep joints causing small-scale greisenisation.

In contrast to layered aplite–pegmatites, layering and UST in Podlesí dyke granite developed near the upper contact and crystallized downwards. Sudden opening of the system followed by rapid decrease of pressure led to undercooling and crystallization of UST. Differences in the nucleation lag time of the major minerals promoted evolution of orthoclase- or zinnwaldite-dominated UST layers. Changes in chemical composition of the boundary layer produced the oscillating mica- and feldspar-rich laminae. The Podlesí granites demonstrate that combination of models of adiabatic fluctuation of pressure (“swinging eutectic”; Balashov et al., 2000) and boundary-layer crystallization of undercooled melt (Webber et al., 1997; London, 1999) can explain the formation of magmatic layering and UST in highly fractionated granitic rocks. However, the accumulation of K in the orthoclase-dominated UST layer, similar to the K accumulation in the upper parts of layered aplite–pegmatites, remains to be resolved.

Acknowledgements

This work has been supported by the state scientific program “Complex geochemical research of interaction and migration of organic and inorganic chemicals in rock environment” supported by the Ministry of the Environment of the Czech Republic by Grant Project No. VaV/3/630/00. We thank many colleagues who supported the investigation of the Podlesí granite system through years, namely J. Frýda and I. Vavřín for technical assistance at the microprobe, and the staff of the chemical laboratory of CGS for the whole-rock analyses. Financial support for A.M. was provided by the Deutsche Forschungsgemeinschaft (MU 1717/2-1) and for J.L. by the Ministry of Education, Youth and Sports of the Czech Republic (MSM J/07-981431000004). D. London and W.D. Sinclair are thanked for detailed revision of the manuscript, which helped us to

improve the article significantly. We are grateful for the improvement of the English to C. Stanley. We are also grateful to O. Tapani Rämö for invitation to take part in the Prof. Haapala celebration meeting and for many inspiring comments and editorial improvement of the manuscript.

Appendix A. Analytical methods

SEM cathodoluminescence and electron microprobe analysis of trace elements in quartz

SEM-CL images were collected from a JEOL 8900 RL electron microprobe at the University of Göttingen with a CL detector (CLD40 R712) using slow beam scan rates of 20 s at processing resolution of 1024×860 pixels and 256 grey levels. The electron beam voltage and current was 30 keV and 200 nA, respectively. Trace element abundances of Al, Ti, K, and Fe in quartz were determined using the same JEOL system which is fitted with five wavelength-dispersive spectrometers. Synthetic Al_2O_3 and TiO_2 , orthoclase, Lucerne, Switzerland and haematite, Rio Marina, Elba, were used as standards. Matrix corrections were made using the phi-rho-z method of Armstrong (1991). Accelerating voltage of 20 kV, beam current of 80 nA, beam diameter of 5 μm , and counting times of 15 s for Si and of 300 s for Ti, K, and Fe were chosen. Limits of detection are 15 ppm for Ti, 11 ppm for K, 15 ppm for Fe, 51 ppm for Na, and 10 ppm for Al. For more explanations, see “Appendix A” in Müller et al. (2002).

Optical cathodoluminescence

The samples were analysed using cathodoluminescence equipment with hot cathode HC₂-LM, Simon Neuser, Bochum, accelerating voltage 14 kV, beam density 10 mA/mm² in the laboratory of Masaryk University Brno and in the laboratory of University of Göttingen.

Whole-rock chemical analyses

Major elements were analysed using standard methods of wet chemistry at the Laboratory of the Czech Geological Survey, Prague. Pb, Rb, Sn, Zn, and

Zr were analysed by XRF at the Laboratory of the Czech Geological Survey; other trace elements were analysed using ICP-MS in ACME Laboratory, Vancouver.

Estimation of Li-content in Li-Fe micas

For the estimation of Li-content in micas analysed by microprobe, we used the equation $\text{Li}_2\text{O (wt.\%)} = 0.335 \times (\text{wt.\% of SiO}_2) - 12.5$, which is based on statistical evaluation of 42 chemically analysed monomineralic mica concentrates from the studied locality. This equation fit in the area of Li-rich micas (>1.5 wt.% Li_2O) better than the equations published by Stone et al. (1988), Tindle and Webb (1990) and Tischendorf et al. (1997), all fitted for micas with much broader interval of Li-contents.

References

- Allman-Ward, P., Halls, C., Rankin, A.H., Bristov, C.M., 1982. An intrusive hydrothermal breccia body at Wheal Remfry in the western part of the St. Austel granite pluton, Cornwall, England. In: Evans, A.M. (Ed.), *Metallization Associated with Acid Magmatism*. John Wiley, London, pp. 1–28.
- Armstrong, J.T., 1991. Quantitative elemental analysis of individual microparticles with electron beam instruments. In: Heinrich, K.F.J., Newbury, D.E. (Eds.), *Electron Probe Quantification*. Plenum, New York, London, pp. 261–315.
- Balashov, V.N., Zaraisky, G.P., Seltmann, R., 2000. Fluid–magma interaction and oscillatory phenomena during crystallization of granitic melt by accumulation and escape of water and fluorine. *Petrology* 8, 505–524.
- Baluj, G.A., 1995. Unique example of layered granitic melts in intrusions in the Coast Zone of the Primorie region. *Doklady Akademii Nauk* 341, 83–88. (in Russian).
- Bardintzeff, J.M., 1999. *Vulkanologie*. Enke, Stuttgart.
- Best, M.G., Christiansen, E.H., 2001. *Igneous Petrology*. Blackwell Science, Malden.
- Breaks, F.W., Moore Jr., J.M., 1992. The Ghost lake batholith, Superior province of northwestern Ontario: a fertile, S-type, peraluminous granite-rare element pegmatite system. *Canadian Mineralogist* 30, 835–875.
- Breiter, K., 2002. From explosive breccia to unidirectional solidification textures: magmatic evolution of a phosphorus- and fluorine-rich granite system (Podlesí, Krušné Hory Mts., Czech Republic). *Bulletin of the Czech Geological Survey* 77, 67–92.
- Breiter, K., Kronz, A., 2003. Chemistry of phosphorus-rich topaz. In: Cempírek, J. (Ed.), *International Symposium on Light Elements in Rock-Forming Minerals, Abstracts*. Masaryk University Brno, pp. 9–10.
- Breiter, K., Frýda, J., Seltmann, R., Thomas, R., 1997. Mineralogical evidence for two magmatic stages in the evolution of an extremely fractionated P-rich rare-metal granite: the Podlesí stock. *Journal of Petrology* 38, 1723–1739.
- Breiter, K., Frýda, J., Leichmann, J., 2002. Phosphorus and rubidium in alkali feldspars: case studies and possible genetic interpretation. *Bulletin of the Czech Geological Survey* 77, 93–104.
- Brigham, R.H., 1983. A fluid dynamic appraisal of a model for the origin of comb layering and orbicular structure. *Journal of Geology* 91, 720–724.
- Cox, R.A., Dempster, T.J., Bell, B.R., Rogers, G., 1996. Crystallization of the Shap granite: evidence from zoned K-feldspar megacrysts. *Journal of the Geological Society* 153, 625–635.
- Cuney, M., Marignac, C., Weisbrod, A., 1992. The Beauvoir topaz-lepidolite albite granite (Massif central, France): the disseminated magmatic Sn–Li–Ta–Nb–Be mineralization. *Economic Geology* 87, 1766–1794.
- Duke, E.F., Papike, J.J., Laul, J.C., 1992. Geochemistry of a boron-rich peraluminous granite pluton: the Calamity Peak layered granite–pegmatite complex, Black Hills, South Dakota. *Canadian Mineralogist* 30, 811–833.
- Eadington, P.J., Nashar, B., 1978. Evidence for the magmatic origin quartz–topaz rocks from the New England batholith, Australia. *Contributions to Mineralogy Petrology* 67, 433–438.
- Fedkin, A., Bezmen, A., Seltmann, R., Zaraisky, G., 2002. Experimental simulation of a layered texture in the F–P-rich granite system. *Bulletin of the Czech Geological Survey* 77, 113–125.
- Fenn, P.M., 1977. The nucleation and growth of alkali feldspars from hydrous melt. *Canadian Mineralogist* 15, 135–161.
- Frindt, S., 2002. *Petrology of the Cretaceous anorogenic Gross Spitzkoppe granite stock, Namibia*. PhD thesis, University of Helsinki, Finland.
- Frýda, J., Breiter, K., 1995. Alkali feldspars as a main phosphorus reservoirs in rare-metal granites: three examples from the Bohemian Massif (Czech Republic). *Terra Nova* 7, 315–320.
- Gottesmann, B., Wasternack, J., Märtens, S., 1994. The Gottesberg tin deposit (Saxony): geological and metallogenic characteristic. In: Seltmann, R., Kämpf, H., Möller, P. (Eds.), *Metallogeny of Collisional Orogens*, Czech Geological Survey, Prague, pp. 110–115.
- Huang, X.L., Wang, R.C., Chen, X.M., Hu, H., Liu, C.S., 2002. Vertical variations in the mineralogy of the Yichun topaz–lepidolite granite Jiangxi province, southern China. *Canadian Mineralogist* 40, 1047–1068.
- Jahns, R.H., Tuttle, O.F., 1963. Layered pegmatite–aplite intrusives. *Mineralogical Society of America Special Paper* 1, 78–92.
- Jahns, R.H., Burnham, C.W., 1969. Experimental studies of pegmatite genesis: I. A model for the derivation and crystallization of granitic pegmatites. *Economic Geology* 64, 843–864.
- Jacquot, Th., 1987. Dynamique de l'organisation séquentielle du magma de Beauvoir. Apport de la pétrologie structurale. In: Cuney, M., Autran, A. *Géologie profonde de la France*

- forage scientifique d'Échassières, vol. 2–3. Géologie de la France, pp. 209–222.
- Jarchovský, T., 1962. Entstehung der Feldspatsäume (Stockscheider) an den Kontakten von Granit- und Greisen-Stöcken im Erzgebirge. *Krystalinikum* 1, 71–80.
- Jarchovský, T., Pavlů, D., 1991. Albite–topaz microgranite from Horní Slavkov (Slavkovský les Mts.) NW Bohemia. *Věstník Ústředního Ústavu Geologického* 66, 13–22.
- Johannes, W., Holz, F., 1996. Petrogenesis and experimental petrology of granitic rocks. *Minerals and Rocks* vol. 22. Springer-Verlag, Berlin.
- Johnston, C., Chappell, B.W., 1992. Topaz-bearing rocks from Mount Gibson, North Queensland, Australia. *American Mineralogist* 77, 303–313.
- Kirkham, R.V., Sinclair, W.D., 1988. Comb quartz layers in felsic intrusions and their relationship to porphyry deposits. In: Taylor, R.P., Strong, D.F. (Eds.), *Recent Advances in the Geology of Granite-Related Mineral Deposits*, Canadian Institute of Mining and Metallurgy, Special Volume, vol. 39, pp. 50–71.
- Kormilicyn, V.S., Manujlova, M.M., 1957. Rhythmic banded quartz porphyry at Bugdai Peak, southeast Transbaykal region. *Zapiski Vsesoyuznovo Mineralogiceskovo Obschestva* 86, 355–364. (in Russian).
- Kovalenko, V.I., Kovalenko, N.I., 1976. Ongonites (topaz-bearing quartz keratophyre)—subvolcanic analogue of rare-metal Li–F granites. *Joint Soviet-Mongolian scientific-research geological expedition. Transaction 15 (Nauka, Moscow, in Russian)*.
- Larsen, R.B., Henderson, I., Ihlen, P.M., Jacamon, F., Flem, B., 2002. Application of trace elements in granitic quartz to unravel petrogenetic links in complex igneous fields: examples from South Norway. In: Parsons, I. (Ed.), *18th General Meeting of the International Mineralogical Association*, 1–6 September 2002, Edinburgh, Scotland. Programme with Abstracts, pp. 261.
- London, D., 1990. Internal differentiation of rare-element pegmatites: a synthesis of recent research. In: Stein, H.J., Hannah, J.L. (Eds.), *Ore-Bearing Granite Systems; Petrogenesis and Mineralizing Processes*, Geological Society of America Special Paper, vol. 246, pp. 35–50.
- London, D., 1992. The application of experimental petrology to the genesis and crystallization of granitic pegmatites. *Canadian Mineralogist* 30, 499–540.
- London, D., 1995. Geochemical features of peraluminous granites, pegmatites, and rhyolites as sources of lithophile metal deposits. In: Thompson, J.F.H. (Ed.), *Magmas, Fluids, and Ore Deposits* vol. 23. Mineralogical Association of Canada Short Course, pp. 175–202.
- London, D., 1996. Granitic pegmatites. *Transaction of the Royal Society in Edinburgh: Earth Sciences* 87, 305–319.
- London, D., 1999. Melt boundary-layers and the growth of pegmatitic textures. *Canadian Mineralogist* 37, 826–827.
- London, D., Morgan, G.B., Hervig, V.I., 1989. Vapor-undersaturated experiments with Macusani glass+H₂O at 200 MPa, and the internal differentiation of granitic pegmatites. *Contributions to Mineralogy and Petrology* 102, 1–17.
- London, D., Morgan, G.B., Babb, V.I., Loomis, H.A., 1993. Behaviour and effect of phosphorus in system Na₂O–K₂O–Al₂O₃–SiO₂–P₂O₅–H₂O at 200 MPa (H₂O). *Contributions to Mineralogy and Petrology* 113, 175–202.
- London, D., Morgan, G.B., Wolf, V.I., 2001. Amblygonite–montebrasite solid solutions as monitors of fluorine in evolved granitic and pegmatitic melts. *American Mineralogist* 86, 225–233.
- Lowenstern, J.B., Sinclair, W.D., 1996. Exsolved magmatic fluid and its role in the formation of comb-layered quartz at the Cretaceous Logtung W–Mo deposit, Yukon Territory, Canada. *Transactions of the Royal Society of Edinburgh. Earth Sciences* 87, 291–303.
- Manning, D.A.C., 1981. The effect of fluorine on liquidus phase relationships in the system Qz–Ab–Or with excess water at 1 kbar. *Contributions to Mineralogy and Petrology* 76, 206–215.
- Maschmeyer, D., Lehmann, G., 1983. A trapped-hole center causing rose coloration in natural quartz. *Zeitschrift für Kristallographie* 163, 181–196.
- Morgan, G.B., London, V.I., 1999. Crystallization of the little three layered pegmatite–aplite dike, Ramona District, California. *Contributions to Mineralogy and Petrology* 136, 310–330.
- Müller, A., Kronz, A., Breiter, K., 2002. Trace elements and growth patterns in quartz: a fingerprint of the evolution of the subvolcanic Podlesí Granite System (Krušné Hory, Czech Republic). *Bulletin of the Czech Geological Survey* 77, 135–145.
- Oelsner, O.W., 1952. Die pegmatitisch-pneumatolitischen Lagerstätten des Erzgebirges mit Ausnahme der Kontaktlagerstätten. *Freiburgerische Forschungshefte* C4. 80 pp.
- Petersen, J.S., Lofgren, G.E., 1986. Lamellar and patchy intergrowths in feldspars; experimental crystallization of eutectic silicates. *American Mineralogist* 71, 343–355.
- Raimbault, L., Cuney, M., Azencott, C., Duthou, J.L., Joron, J.L., 1995. Geochemical evidence for a multistage magmatic genesis of Ta–Sn–Li mineralization in the granite at Beauvoir. *French Massif Central. Economic Geology* 90, 548–596.
- Rockhold, J.R., Nabelek, P.I., Glascock, M.D., 1987. Origin of rhythmic layering in the Calamity Peak satellite pluton of the Harney Peak granite, South Dakota: the role of boron. *Geochimica et Cosmochimica Acta* 51, 487–496.
- Schust, F., Wasternack, J., 1972. Über das Auftreten von Schlotförmigen Brekzienkörpern bei Gottesberg und Mühlleithen im Granitmassiv von Eibenstock, Erzgebirge. *Zeitschrift für angewandte Geologie* 18, 400–410.
- Seltmann, R., 1994. Sub-volcanic minor intrusions in the Altenberg caldera and their metallogeny. In: Seltmann, R., Kämpf, H., Möller, P. (Eds.), *Metallogeny of Collisional Orogens*. Czech Geological Survey, Prague, pp. 198–206.
- Seltmann, R., Schilka, W., 1991. Metallogenic aspects of breccia-related tin granites in the eastern Erzgebirge. *Zeitschrift für geologische Wissenschaften* 19, 485–490.
- Shannon, J.R., Walker, B.M., Carten, R.B., Geraghty, E.P., 1982. Unidirectional solidification textures and their significance in determining relative ages of intrusions at the Hederson Mine, Colorado. *Geology* 10, 293–297.
- Sillitoe, R.H., 1985. Ore-related breccias in volcanoplutonic arcs. *Economic Geology* 80, 1467–1514.

- Stone, M., Exley, C.S., George, M.C., 1988. Compositions of trioctahedral micas in the Cornubian batholith. *Mineralogical Magazine* 52, 175–192.
- Sykes, M.L., Holloway, J.R., 1987. Evolution of granitic magmas during ascent: a phase equilibrium model. In: Mysen, B.O. (Ed.), *Magmatic Processes: Physicochemical Principles*, Geochemical Society Special Publication, vol. 1, pp. 447–461.
- Taylor, M.C., Sheppard, J.B., Walker, J.N., Kleck, W.D., Wise, M.A., 2002. Petrogenesis of rare-element granitic pegmatites: a new approach. In: Parsons, I. (Ed.), 18th General Meeting of the International Mineralogical Association, 1–6 September 2002, Edinburgh, Scotland. Programme with Abstracts, pp. 260.
- Thomas, R., Förster, H.-J., Heinrich, W., 2003. The behaviour of boron in a peraluminous granite–pegmatite system and associated hydrothermal solutions: a melt and fluid-inclusion study. *Contributions to Mineralogy and Petrology* 144, 457–472.
- Tindle, A.G., Webb, P.C., 1990. Estimation of lithium contents in trioctahedral micas using microprobe data: application to micas from granitic rocks. *European Journal of Mineralogy* 2, 595–610.
- Tischendorf, G., Gottesmann, B., Förster, H.-J., Trumbull, R.B., 1997. On Li-bearing micas: estimation Li from electron microprobe analyses and an improved diagram for graphical representation. *Mineralogical Magazine* 61, 809–834.
- Webber, K.L., Falster, A.U., Simmons, W.B., Ford, E.E., 1997. The role of diffusion-controlled oscillatory nucleation in the formation of line rock in pegmatite–aplite dikes. *Journal of Petrology* 38, 1777–1791.
- Webber, K.L., Simmons, W.B., Falster, A.U., Ford, E.E., 1999. Cooling rates and crystallization dynamics of shallow level pegmatite–aplite dikes, San Diego County, California. *American Mineralogist* 84, 708–717.
- Weiss, Z., Rieder, M., Smrčok, L., Petříček, V., Bailey, S.W., 1993. Refinement of the crystal structures of two “protolithionites”. *European Journal of Mineralogy* 5, 493–502.
- Wolf, M.B., London, D., 1997. Boron in granitic magmas: stability of tourmaline in equilibrium with biotite and cordierite. *Contributions to Mineralogy and Petrology* 130, 12–30.
- Xiong, X.L., Zhao, Z.H., Zhu, J.C., Rao, B., 1999. Phase relations in albite granite–H₂O–HF system and their petrogenetic application. *Geochemical Journal* 33, 199–214.
- Žák, K., Pudilová, M., Breiter, K., 2001. Oxygen isotope study of the highly fractionated Podlesí granite system—preliminary data. In: Breiter, K. (Ed.), *International Workshop Phosphorus- and Fluorine-rich Fractionated Granites, Podlesí*. Czech Geological Survey, Praha, pp. 34–35.
- Zaraisky, G.P., Seltmann, R., Shatov, V.V., Aksyuk, A.M., Shapovalov, Yu.B., Chevychelov, V.Yu., 1997. Petrography and geochemistry of Li–F granites and pegmatite–aplite banded rocks from the Orlovka and Etyka tantalum deposits in Eastern Transbaikalia, Russia. In: Papunen, H. (Ed.), *Mineral Deposits*. Balkema, Rotterdam, pp. 695–698.